Systemic Administration of the Benzodiazepine Receptor Partial Inverse Agonist FG-7142 Disrupts Corticolimbic Network Interactions

CARL W. STEVENSON,[1][*] **DAVID M. HALLIDAY,**[2] **CHARLES A. MARSDEN,**[1] AND **ROB MASON**[1]
[1]*School of Biomedical Sciences, University of Nottingham, Nottingham, United Kingdom*
[2]*Department of Electronics, University of York, York, United Kingdom*

ABSTRACT   The medial prefrontal cortex (mPFC) and basolateral amygdala (BLA) coordinate various stress responses. Although the effects of stressors on mPFC and BLA activity have been previously examined, it remains unclear to what extent stressors affect functional interactions between these regions. In vivo electrophysiology in the anesthetized rat was used to examine mPFC and BLA activity simultaneously in response to FG-7142, a benzodiazepine receptor partial inverse agonist that mimics various stress responses, in an attempt to model the effects of stressors on corticolimbic functional connectivity. Extracellular unit and local field potential (LFP) recordings, using multielectrode arrays positioned in mPFC and BLA, were conducted under basal conditions and in response to systemic FG-7142 administration. This drug increased mPFC and BLA unit firing at the lowest dose tested, whereas higher doses of FG-7142 decreased various burst firing parameters in both regions. Moreover, LFP power was attenuated at lower (<1 Hz) and potentiated at higher frequencies in mPFC (1–12 Hz) and BLA (4–8 Hz). Interestingly, FG-7142 diminished synchronized unit firing, both within and between mPFC and BLA. Finally, FG-7142 decreased LFP synchronization between these regions. In a separate group of animals, pretreatment with the selective benzodiazepine receptor antagonist flumazenil blocked the changes in burst firing, LFP power and synchronized activity induced by FG-7142, confirming direct benzodiazepine receptor-mediated effects. These results indicate that FG-7142 disrupts corticolimbic network interactions via benzodiazepine receptor partial inverse agonism. Perturbation of mPFC-BLA functional connectivity induced by FG-7142 may provide a useful model of corticolimbic dysfunction induced by stressors. **Synapse 61:646–663, 2007.**   © 2007 Wiley-Liss, Inc.

INTRODUCTION

Gene–environment interactions are thought to mediate the development of mental illness (Cooper, 2001; Nemeroff and Vale, 2005). Stress is arguably the most important environmental factor involved, as symptom exacerbation and provocation are induced by stressors in several psychiatric diseases, including mood disorders (Battaglia and Ogliari, 2005; McEwen, 2000). Furthermore, these disorders are characterized by dysfunction of the prefrontal cortex (PFC) and amygdala (Davidson et al., 2002; Drevets, 2001; Gilboa et al., 2004; Shin et al., 2004), brain regions which mediate cognitive and emotional regulation (LeDoux, 2000; Robbins, 2000) and, as such, are

involved in coordinating various stress responses (Buijs and van Eden, 2000).

Indeed, rodent studies indicate that the medial prefrontal cortex (mPFC) and basolateral amygdala (BLA) are activated by various stressors (Beck and Fibiger, 1995; Duncan et al., 1993). These areas share reciprocal connections (McDonald, 1991, 1998) and evidence from combined stimulation and in vivo electro-

*Correspondence to: Carl W. Stevenson, PhD, Leicester School of Pharmacy, De Montfort University, Hawthorn Building, The Gateway, Leicester LE1 9BH, United Kingdom. E-mail: cstevenson@dmu.ac.uk

physiology studies indicates that these connections are functionally relevant. Electrical stimulation of BLA inhibits spontaneous activity in mPFC projection neurons, possibly by activating local GABA interneurons (Pérez-Jaranay and Vives, 1991). Similarly, mPFC stimulation reduces the firing rate of BLA projection neurons, presumably by activating either local GABA interneurons (Rosenkranz and Grace, 2001, 2002) or inhibitory recurrent collaterals of neighboring intercalated cells (Smith et al., 2000).

The functional connectivity between mPFC and BLA is also relevant in processing sensory input related to stressful stimuli. Conditioned stressors alter activity in mPFC neurons and this effect is abolished by lesions (Garcia et al., 1999) or pharmacological inactivation (Laviolette et al., 2005) of BLA. Unconditioned stress also blocks long-term potentiation in mPFC, an effect mimicked by BLA stimulation (Maroun and Richter-Levin, 2003). Moreover, conditioned stressor-induced activity and plasticity in BLA neurons is suppressed by concurrent mPFC stimulation (Rosenkranz et al., 2003). However, few studies have investigated functional interactions between mPFC and BLA directly by examining neuronal activity in both regions simultaneously in response to stressful stimuli.

In an attempt to model the effects of stressors on mPFC-BLA functional connectivity, this study examined extracellular multi-unit and local field potential (LFP) activity concurrently in mPFC and BLA, in the anesthetized rat, in response to systemic administration of FG-7142. This benzodiazepine receptor partial inverse agonist mimics various behavioral, neuroendocrine, and autonomic stress responses. For example, FG-7142 causes anxiety (File et al., 1982, 1985; Pellow and File, 1986), impairs working memory (Birnbaum et al., 1999; Murphy et al., 1996), induces corticosterone release (Pellow and File, 1985; Stephens et al., 1987) and potentiates sympathetic arousal (Berntson et al., 1996; Hart et al., 1998). As is the case with other stressors, FG-7142 also increases monoamine metabolism (Bradberry et al., 1991; Dazzi et al., 2002; Ida et al., 1991) and Fos activation (Kurumaji et al., 2003; Singewald et al., 2003) in mPFC and BLA. To determine if the effects of FG-7142 were mediated specifically by benzodiazepine receptor partial inverse agonism, a separate group of animals undergoing electrophysiological recordings in mPFC and BLA were pretreated with the selective benzodiazepine receptor antagonist flumazenil (FLU) prior to FG-7142 administration.

MATERIALS AND METHODS
Animals

All experiments were performed on male Lister hooded rats (300–400 g) bred in the Biomedical Serv-ices Unit, University of Nottingham Medical School. Animals were housed 3–4 per cage on a 12-h light/dark cycle (lights on at 0700 h) with free access to food and water. All experimental procedures were carried out in accordance with the Animals (Scientific Procedures) Act 1986, UK.

Surgery

All drugs and chemicals were obtained from Sigma (MO) unless otherwise stated. Anesthesia was induced with 3.5% isoflurane (IVAX Pharmaceuticals, UK) in a 50% N_2O:50% O_2 mixture (BOC Gases, UK). The isoflurane level was reduced progressively and maintained at 2.0% throughout surgery to ensure complete inhibition of the hindpaw withdrawal reflex. Body temperature was monitored and maintained at $\sim37°C$, using a homeothermic heating pad (Harvard Apparatus, UK). The femoral vein was cannulated with portex fine bore polythene tubing (0.28 mm ID; Scientific Laboratory Supplies, UK) for i.v. administration of drug (see below) prior to placing the animal in a stereotaxic frame. The incisor bar was adjusted to maintain the skull horizontal and a scalp incision was made. Separate craniotomies (~2 mm diameter) were performed over the right mPFC and BLA. The dura mater was excised and the underlying cortex was kept moist with 0.9% sodium chloride. Two eight-microwire electrode arrays (NB Labs, TX), configured as bundles, were used to record unit and LFP activity from multiple neurons simultaneously in mPFC and BLA. Electrode arrays were lowered into the right ventral prelimbic/infralimbic cortex (3.0 mm anterior and 0.5–0.7 mm lateral to bregma; 3.8–4.2 mm ventral to the cortical surface) and basal amygdaloid nucleus (2.8 mm posterior and 4.8–5.0 mm lateral to bregma; 7.7–8.0 mm ventral to the surface of the brain), using the atlas coordinates of Paxinos and Watson (1997).

Recording procedure

Microwire electrodes (Teflon-coated stainless steel, 50 μm diameter/wire, NB Labs, TX) had an impedance of ~100 kΩ measured at 1 kHz (Robinson, 1968). Electrode arrays were connected via a unity-gain multichannel headstage (HST/8m-G1, Plexon, TX) to a multichannel preamplifier. Extracellular action potential spikes and LFPs [gain 1000×; band-pass filtered at 250–8 kHz (spikes) and 0.7–170 Hz (LFPs); Plexon] were fed to a Plexon Multichannel Acquisition Processor (MAP) Box linked to a host PC (Dell 1.5 GHz; Windows 2000), providing simultaneous 40 kHz (25 μs) A/D conversion on each channel at 12-bit resolution. The MAP system provided further additional programmable amplification and filtering of spikes (final gain up to 32000×, final bandwidth 400–5 kHz). Unit activity was displayed on D11 5000

series dual-beam (Tektronix, OR) and 507 analog-digital (Hameg Instruments, Germany) oscilloscopes and also monitored aurally with the aid of a loudspeaker. LFP signals were digitized at 1 kHz.

Drug administration

Electrode arrays were allowed to settle for ~30 min after being lowered into the mPFC and BLA prior to recording basal activity for 20–30 min in each region. Following basal recordings, animals received repeated systemic (i.v.) injections of FG-7142. In one group of animals, vehicle (10% cremophor EL in 0.5 ml/kg; Hart et al., 1998) and four doses of FG-7142 (0.33, 1.0, 3.3, 10.0 mg/kg in 0.5 ml/kg) were each injected every 3 min. The higher doses in the range used here are comparable to those used in previous studies examining the effects on anxiety-related behavior (Berntson et al., 1996; Birnbaum et al., 1999; File et al., 1982, 1985; Hart et al., 1998; Murphy et al., 1996; Pellow and File, 1985, 1986; Stephens et al., 1987). Each dose was followed immediately by injection of heparinized saline (50 μl; CP Pharmaceuticals, UK) to flush the cannula and thus ensure that drug was administered completely. Drug and saline administration combined occurred over 30 s. In another group, after vehicle injection, animals were pretreated with FLU (1.0 mg/kg, i.v. in 0.5 ml/kg; Tocris, UK) prior to FG-7142 injection (10.0 mg/kg). Again, drug injections occurred every 3 min and each was followed immediately by an injection of heparinized saline.

Histology

At the end of each experiment, current (0.1 mA) was passed through random pairs of microwires in each electrode array for 5–7 s to deposit ferric ions at the electrode tips. Isoflurane levels were then increased to 5% to ensure deep anesthesia prior transcardial perfusion with 0.9% NaCl followed by a 4% paraformaldehyde/4% potassium ferrocyanide solution. Brains were removed and stored in perfusion medium until sliced. Ferrocyanide reacts with the deposited iron to produce a Prussian blue reaction at the electrode tips (Green, 1958). Brains were sectioned (200 μm) with a vibratome (Camden Instruments, UK) and stained for acetylcholinesterase (0.021 M acetylthiocholine iodide, 0.2 M sodium phosphate monobasic, 0.6 M sodium citrate, 0.06 M cupric sulfate, 0.01 M potassium ferricyanide) to determine electrode array placements within mPFC and BLA.

Data analysis

Spike sorting

Spike discrimination was achieved with Off-Line Sorter software (Plexon), using both automatic and manual sorting techniques. Principle component analysis was used to display the waveforms recorded from each electrode in three-dimensional space. Each electrode was checked for artifacts (e.g., noise) which were removed manually. Automatic sorting (valley-seeking) methods were then used to separate the waveforms into individual units. The resulting clusters were inspected and the units were considered to be separate only if the cluster borders did not overlap. Furthermore, waveforms which were not consistent with the shape of action potentials and occurred within the absolute refractory period (1.1 ms; Homayoun et al., 2005; Jackson et al., 2004) were also manually removed. Finally, clusters were considered to be single units only if the autocorrelogram showed that no significant errors occurred in sorting as a result of noise and if the firing rate during the final 150 s of the baseline period was >0.1 Hz (Kim et al., 2001). Although most electrodes only had one discriminated unit, up to 3 units were observed on some electrodes.

mPFC neurons

Neuronal subtypes in mPFC have previously been characterized based on differences in firing rate and action potential waveform characteristics. Studies have shown that regular-spiking neurons, presumed to be pyramidal cells, have a firing rate < 10 Hz whereas fast-spiking neurons, presumed to be interneurons, fire at a rate > 10 Hz (Homayoun et al., 2005; Jung et al., 1998; Laviolette et al., 2005). None of the neurons recorded from mPFC had firing rates > 10 Hz and were all therefore initially presumed to be pyramidal cells. Evidence from studies in which fine-tip glass electrodes were used to record neuronal activity also indicates that the majority of mPFC neurons have a biphasic waveform, with an initial negative deflection followed by a positive deflection in the action potential waveform; it is presumed that these neurons are pyramidal cells. The remaining neurons show triphasic waveforms, with a small positive deflection preceding the initial negative deflection, and are presumed to be interneurons (Gronier and Rasmussen, 2003; Sesack and Bunney, 1989). Given that electrophysiological recordings in the present study were conducted using metal wires and not fine tip glass electrodes, the utility of using these waveform criteria to classify neuronal subtypes may be limited. Nevertheless, examination of the average waveform shape (first 500 waveforms of each unit; data not shown) of the units recorded in the present study revealed that all but two of the neurons exhibited waveform characteristics consistent with pyramidal cells; the two which were putatively characterized as interneurons were omitted from the data analysis. A paucity of recordings from interneurons in mPFC

has been observed in other studies (Homayoun et al., 2005; Jackson et al., 2004; Laviolette et al., 2005) and is likely due to both anatomical and technical considerations. Anatomical studies indicate that the majority of neurons in mPFC are pyramidal cells (Gabbott et al., 1997). Furthermore, the large diameter (50 μm) metal electrodes used in the present study preferentially detect activity in larger pyramidal cells when compared with smaller interneurons (Snodderly, 1973).

BLA neurons

Characterization of distinct subtypes of BLA neurons is also possible based on differences in basal firing rate and action potential duration. Again, two distinct neuronal populations have been identified in BLA such that fast-firing neurons with short duration action potentials are presumed to be interneurons, whereas slow-firing neurons with long duration action potentials are thought to be pyramidal cells (Pistis et al., 2004; Rosenkranz and Grace, 1999). However, examination of basal firing rate and action potential duration of units recorded in the present study did not show any obvious relationship between these two parameters, suggesting that the majority of units were of the same neuronal subtype. Thus, given that most neurons in BLA are pyramidal cells (McDonald and Mascagni, 2001), and that the electrodes used in the present study detect activity preferentially from larger neurons (Snodderly, 1973), it is tempting to speculate that the majority of BLA units recorded from in the present study were pyramidal cells. Although previous studies of BLA unit recordings have not used waveform shape as a criterion in determining the neuronal subtype in this region, the four BLA neurons which exhibited triphasic waveforms in the present study were omitted from the data analysis.

Firing rate

Electrophysiological data were analyzed using NeuroExplorer (TX). Basal firing rate was defined as the average firing rate (Hz) during the final 150 s of the baseline recording period (i.e., immediately preceding vehicle infusion). The effects of vehicle injection on basal firing rate in mPFC and BLA were determined separately, using paired t-tests. Given that i.v. administration of FG-7142, or FLU pretreatment followed by FG-7142, had immediate and sustained effects on unit and LFP activity, average firing rate was determined for the 150 s period immediately following vehicle or drug injection. The effects of increasing dose of FG-7142 were expressed as a percentage of vehicle (±SEM) and were compared separately in mPFC and BLA using a one-way analysis of variance (ANOVA),
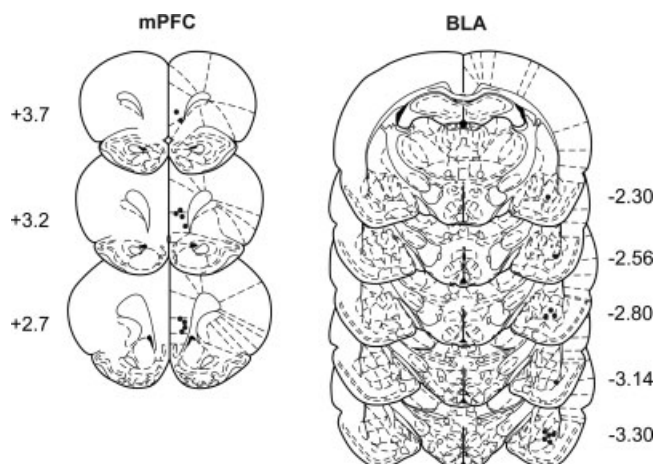

Fig. 1. Schematic representation of multi-electrode array placements within mPFC and BLA. The distance (mm) anterior (mPFC) or posterior (BLA) to bregma is indicated beside each coronal section (Paxinos and Watson, 1997).

with dose as the within-subject factor. Similarly, the effects of FLU pretreatment on FG-7142-induced changes in firing rate were analyzed separately in mPFC and BLA using a one-way ANOVA, again with drug as the within-subject factor. Post hoc comparisons were performed using Tukey's Honestly Significant Difference (HSD) test.

Burst firing parameters

There are two widely accepted methods of examining burst firing parameters based on differences in the interstimulus interval (ISI) distribution of unit firing (Homayoun et al., 2005). In the histogram method, ISI histograms are used to determine the distribution of burst ISIs when compared with other ISIs in a given spike train (Cocatre-Zielgien and Delcomyn, 1992). However, this method, often used for detecting regular bursting patterns seen in tonically firing neurons, does not detect bursts with highly variable ISIs (Kaneoke and Vitek, 1996). In the Poisson surprise method, bursts are defined as groups of spikes whereby successive ISIs in a given spike train do not follow a Poisson distribution based on the mean firing rate of the spike train (Boraud et al., 2002; Legendy and Salcman, 1985). Bursts are thus detected by locating consecutive ISIs of less than half the mean ISI and then testing whether they would be expected if the spike train followed a Poisson distribution (Homayoun et al., 2005). In the present study, both mPFC and BLA units displayed an irregular activity pattern characterized by periods of low tonic activity coupled with phasic burst firing, therefore the Poisson surprise method of burst detection was used to analyze burst firing parameters.
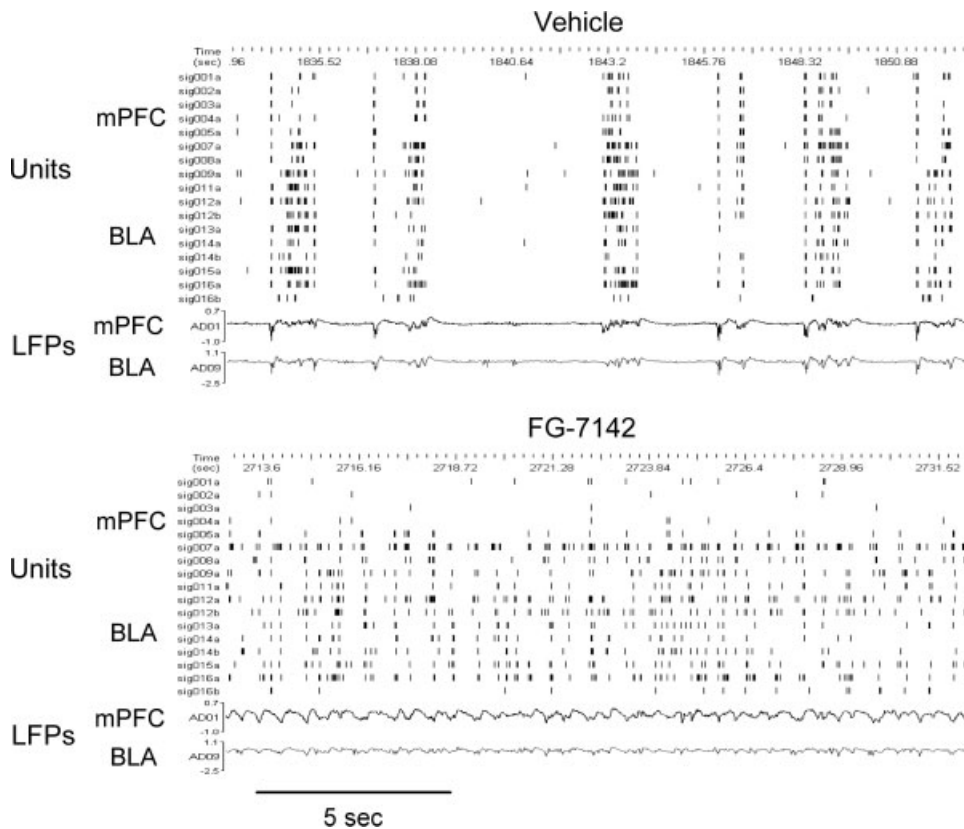
Fig. 2. Representative mPFC and BLA unit rasters and LFP plots from one experiment, in response to vehicle and FG-7142 (10.0 mg/kg) injection. The top seven raster plots correspond to discriminated mPFC units and the bottom 10 rasters represent distinct BLA units (20 s). In response to vehicle, units displayed correlated activity characterized by irregular burst firing. In contrast, units exhibited less correlated activity in response to FG-7142. Similarly, LFPs showed irregular activity in response to vehicle whereas an oscillatory pattern of activity emerged after FG-7142 administration.

The surprise value used in the Poisson surprise method can be defined as the negative natural logarithm of the probability that a series of spikes in a given time interval is significantly different from that expected from a Poisson process with the same mean firing rate (Homayoun et al., 2005; Legendy and Salcman, 1985). The surprise value provides an estimate of the statistical significance of the burst detection. In the present study a surprise value of three was used, indicating that bursts occur ∼20 times ($P < 0.05$) more frequently than would be expected in a Poisson distribution with the same mean firing rate (Homayoun et al., 2005). The burst parameters measured (NeuroExplorer) were the number of bursts occurring per minute (bursts/min), the percentage of spikes firing in bursts and the number of spikes occurring in each burst (spikes/burst). The effects of FG-7142 dose on each burst parameter during the 150 s period immediately following injection were compared with vehicle. Similarly, the effects of FLU and FG-7142 on bursting parameters during the 150 s period immediately following drug injection were compared with vehicle. Each burst parameter was analyzed separately in mPFC and BLA using a one-way ANOVA, with dose (FG-7142) or drug (FLU pretreatment) as the within-subject factor. Again, post hoc comparisons were performed using Tukey's HSD test.

LFP activity

The LFP can be considered the vector sum of all (i.e., dendritic, somatic, axonal, synaptic) electrical activity in a relatively large volume (up to 1 mm^3) and is therefore attributable to both pre- and postsynaptic activity in many neurons in a given region (Bullock, 1997). Power spectra were generated from the 150 s epochs associated with each dose of FG-7142, using periodogram-based spectral estimation techniques (Halliday et al., 1995). Power spectra were also generated in response to administration of vehicle, FLU and FG-7142 in the antagonist pretreatment experiment. Comparisons between the effects of vehicle and FG-7142 (10.0 mg/kg), or FG-7142 and FLU, on signal power were made using a log ratio comparison of spectra test (Diggle, 1990). Confidence intervals (95%) for these ratios were used to characterize any statistically significant differences in power between conditions.

Coherence analysis

Coherence is a measure of linear association between two signals (units and/or LFPs) in the frequency domain (Halliday et al., 1995). This measure is dimensionless and is bounded from 0 to 1; a value of zero indicates no linear relationship and a value of one indicates two identical signals at a particular frequency. Coherence spectra were calculated from the

mPFC

BLA

Fig. 3. Effects of FG-7142 on firing rate. FG-7142 significantly increased the mean firing rate of mPFC and BLA neurons but only at the lowest dose (0.33 mg/kg) tested (* 0.33 vs. VEH, 1.0, 3.3, and 10.0 mg/kg, $P < 0.01$).
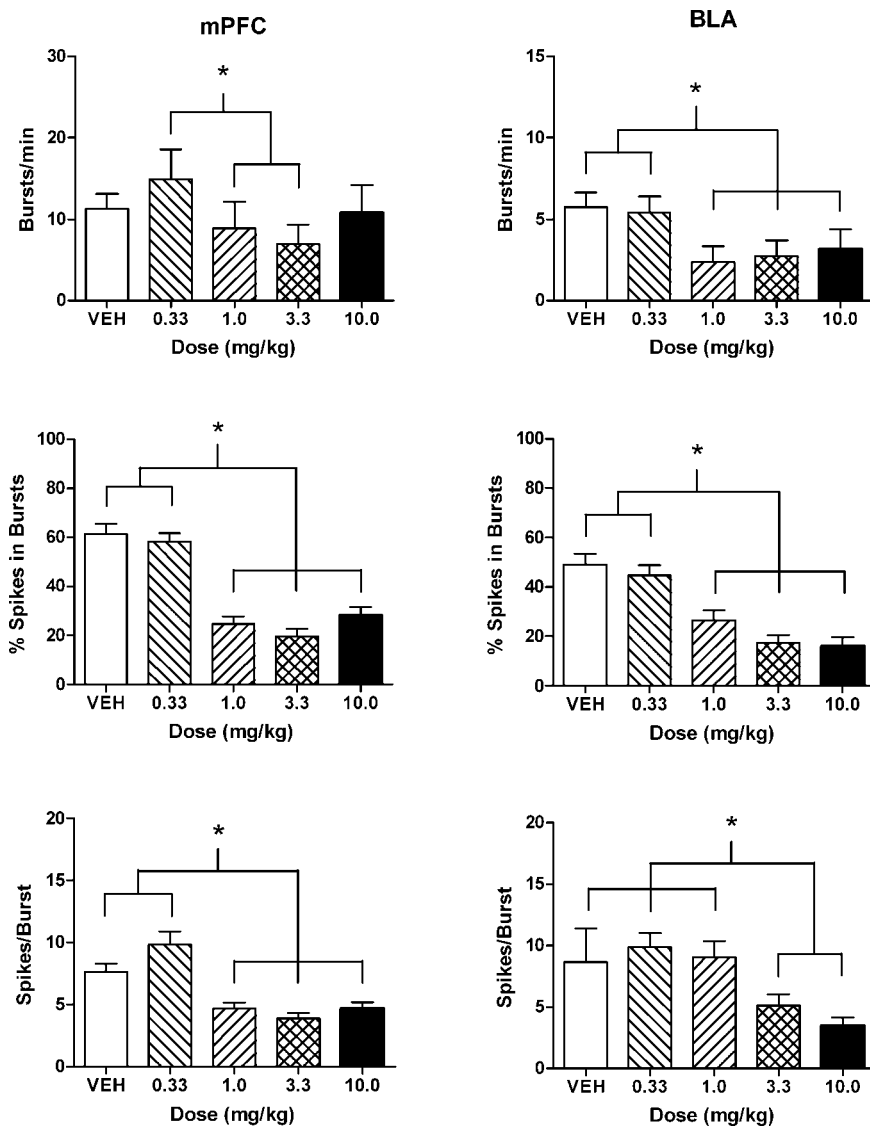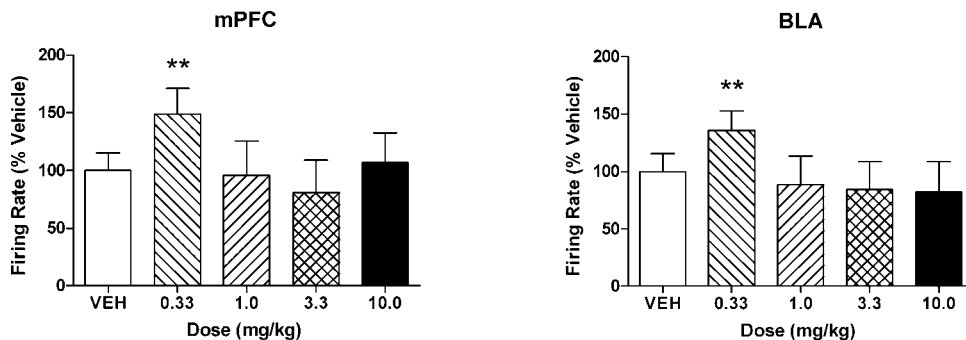
mPFC

BLA

Fig. 4. Effects of FG-7142 on burst firing parameters. In contrast to its effects on firing rate, FG-7142 decreased mPFC and BLA burst firing at the higher doses tested. In mPFC, FG-7142 significantly decreased the percentage of spikes firing in bursts and the mean number of spikes/burst at higher doses (* Vehicle and 0.33 vs. 1.0, 3.3, and 10.0 mg/kg, $P < 0.05$). In BLA, FG-7142 significantly decreased the mean number of bursts/min (* Vehicle and 0.33 vs. 1.0, 3.3, and 10.0 mg/kg, $P < 0.05$), percentage of spikes firing in bursts (* Vehicle and 0.33 vs. 1.0, 3.3, and 10.0 mg/kg, $P < 0.05$) and the mean number of spikes/burst (* Vehicle, 0.33 and 1.0 vs. 3.3 and 10.0 mg/kg).

periodogram-based spectral estimates described earlier, and pairwise comparisons (unit or LFPs) corresponding to FG-7142 dose, or FG-7142 and FLU in the antagonist experiment, were generated by dividing the experimental records into a number of sections of equal duration (150 s). Coherence spectra for a random pair of mPFC neurons, a random pair of BLA neurons and one random unit in each of mPFC and BLA were generated from each animal. Individual coherence spectra were then combined across animals to give pooled coherence estimates that examine the functional coupling of unit activity within mPFC,

within BLA, or between mPFC and BLA across the population of animals in each group (Amjad et al., 1997). LFP coherence spectra from each experiment were also combined across animals in the same manner. Comparisons between the effects of vehicle and FG-7142 (10.0 mg/kg), or FG-7142 and FLU, on pooled coherence were undertaken using a comparison of coherence test (Rosenberg et al., 1989). Confidence intervals (95%) for these comparisons were used to examine any statistically significant differences in unit (mPFC-mPFC, BLA-BLA, mPFC-BLA) or LFP coherence.

Cumulant density analysis

Time domain analysis of correlation between units or LFPs was undertaken using cumulant density estimates (Halliday et al., 1995). These provide a measure of correlation and have a similar interpretation to cross-correlation functions. Cumulant density estimates were constructed from the same cross-spectral estimates described earlier. The expected value of cumulant density estimates for uncorrelated signals is zero. Upper and lower 95% confidence intervals were used to indicate the presence of significant departures from zero at a particular time lead or lag. Cumulant densities were calculated for the same pairs of neurons and using the same data as the coherence estimates described earlier. Cumulant densities were also computed for LFPs in mPFC and BLA from the same data segments as the corresponding coherence estimates. Cumulant densities from each experiment were then combined across animals to examine the correlation of unit activity within mPFC, within BLA, or between mPFC and BLA. Differences in cumulant density were examined qualitatively in response to varying doses of FG-7142 or the effects of FG-7142 after prior FLU pretreatment. MATLAB scripts for the spectral, coherence, and cumulant density analysis are available from www.neurospec.org.

RESULTS

The location of multi-electrode arrays within the mPFC and BLA are illustrated in Figure 1. Only animals with histologically-confirmed placements in mPFC (ventral prelimbic or infralimbic cortices) or BLA (basal nucleus) were included in the data analysis. Six rats in the FG-7142 group and four rats in the FLU pretreatment group met histological criteria.

Multiple unit and LFP activity in mPFC and BLA from one experiment are shown in Figure 2. Neurons in both regions exhibited an irregular firing pattern characterized by periods of very low tonic activity coupled with phasic burst firing. This pattern of activity has been reported by others conducting in vivo extracellular recordings from mPFC (Gronier and Rasmussen, 2003; Homayoun et al., 2005; Jackson
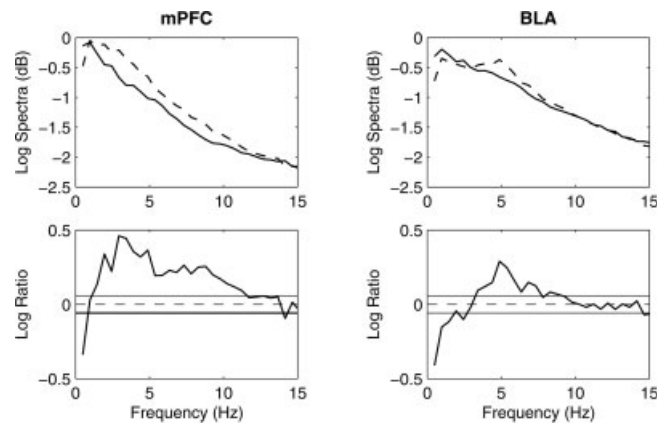

Fig. 5. Effects of FG-7142 on LFP activity. The upper plots show log spectral estimates with vehicle and FG-7142 (10.0 mg/kg) represented by solid and dashed lines, respectively (data for lower doses of FG-7142 not shown). The lower plots show the log ratio test for comparison of the two spectra; the two solid horizontal lines indicate the upper and lower 95% confidence limits (vehicle is the reference signal in the comparison). In mPFC, FG-7142 significantly decreased LFP power at the lowest frequencies (<1 Hz) and significantly increased power in the delta (1–4 Hz), theta (4–8 Hz) and alpha (8–12 Hz) bands, compared with vehicle. Similarly, in BLA, FG-7142 significantly decreased power at low (<1 Hz) frequencies and significantly increased power in the theta band, compared with vehicle.

et al., 2004) and BLA (Ponomarenko et al., 2003) neurons in the rat. The LFP activity pattern mirrored that of neuronal firing in each region such that the initial negative deflection in potential coincided with neuronal bursting in mPFC and BLA. This temporal association between unit and LFP activity has been reported previously in both cortical and amygdaloid regions (Collins et al., 2001; Steriade, 1997). It should be noted that the low frequency LFP activity seen under basal conditions and in response to vehicle is not due to true slow wave oscillations but rather to the "average" of high frequency activity of short duration and the very low activity periods of longer duration observed during the 150 s epoch.

Effects of FG-7142 on unit firing rate

In the animals treated with increasing doses of FG-7142, neurons in mPFC ($n = 41$) and BLA ($n = 40$) had mean (±SEM) firing rates of 1.95 ± 0.26 Hz and 1.13 ± 0.15 Hz, respectively, during the basal recording period. Vehicle had a modest, albeit significant, effect on basal firing rate in mPFC (2.15 ± 0.33 Hz; $t_{(40)} = 2.10$, $P = 0.042$) but not BLA (1.24 ± 0.19 Hz; $t_{(39)} = 1.43$, $P = 0.16$) neurons. The effects of FG-7142 on unit firing rate are represented in Figure 3. FG-7142 increased the mean firing rate of mPFC ($F_{(4,40)} = 8.33$, $P < 0.0001$) and BLA ($F_{(4,39)} = 10.5$, $P < 0.0001$) neurons. However, post hoc analysis revealed that the mean firing rates of both mPFC and BLA neurons were significantly increased only at the
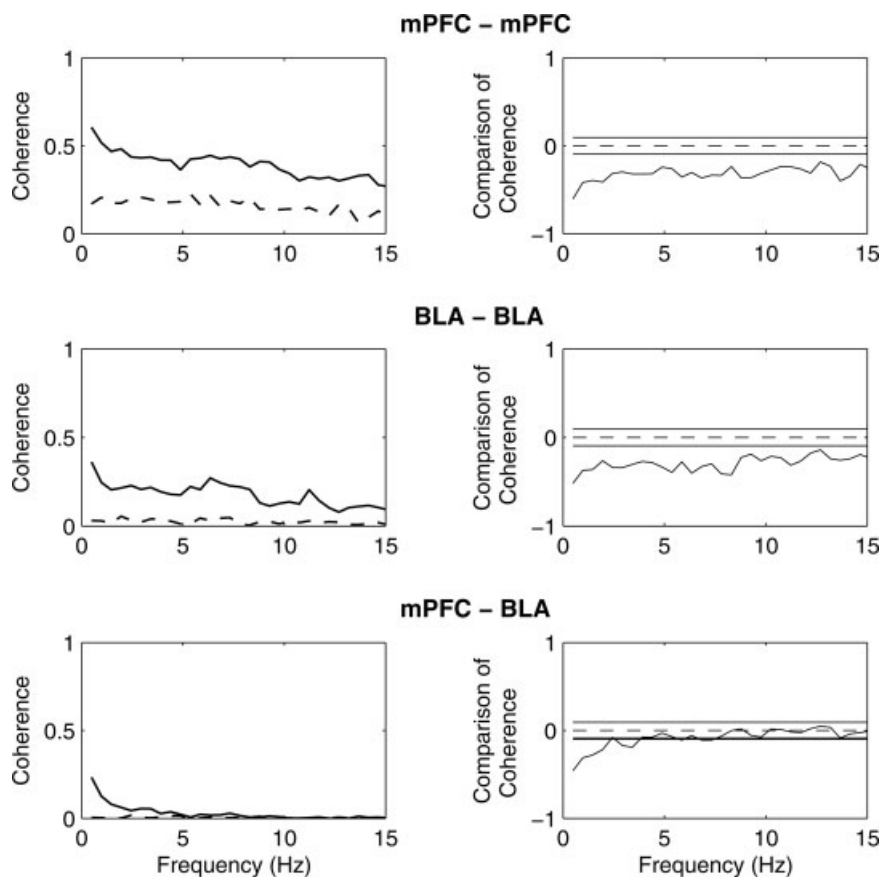
Fig. 6. Effects of FG-7142 on unit coherence. The left column shows coherence plots, where vehicle and FG-7142 are represented by solid and dashed lines, respectively (data for lower doses of FG-7142 not shown). Units within mPFC (mPFC-mPFC) or BLA (BLA-BLA) showed coherence in response to vehicle across the frequency range (0–15 Hz) displayed. However, coherence between units in mPFC and BLA (mPFC-BLA) was observed only at lower frequencies (<8 Hz). The right column illustrates the difference of coherence test, with coherence in the vehicle condition as the reference. The solid horizontal lines on the comparison of coherence graphs represent the upper and lower 95% confidence limits, based on the hypothesis of equal coherence values. Within mPFC or BLA, there was a significant decrease in unit coherence in response to FG-7142, compared with vehicle, across the whole frequency range. Moreover, unit coherence between mPFC and BLA was abolished by FG-7142.

lowest (0.33 mg/kg) dose, compared with vehicle ($P <$ 0.05).

FG-7142 decreases unit burst firing

Figure 4 shows the effects of FG-7142 on various burst firing parameters in mPFC and BLA neurons. In contrast to its effects on firing rate, FG-7142 decreased mPFC and BLA burst firing parameters at the higher doses tested. In mPFC, the percentage of spikes firing in bursts ($F_{(4,40)} = 62.18$, $P < 0.0001$) and mean number of spikes/burst ($F_{(4,40)} = 17.28$, $P < 0.0001$) were significantly decreased at 1.0, 3.3 and 10.0 mg/kg, compared with vehicle ($P < 0.05$). Similarly, in BLA the mean number of bursts/min ($F_{(4,39)} = 7.26$, $P < 0.0001$) and percentage of spikes firing in bursts ($F_{(4,39)} = 30.27$, $P < 0.0001$) were significantly decreased at 1.0, 3.3, and 10.0 mg/kg, compared with vehicle ($P < 0.05$). The mean number of spikes/burst ($F_{(4,39)} = 4.81$, $P < 0.002$) was also significantly decreased at 3.3 and 10.0 mg/kg, compared with vehicle ($P < 0.05$), in BLA.

FG-7142 alters LFP activity

The effects of FG-7142 on LFP activity in mPFC and BLA are represented in Figure 5. In general,

FG-7142 decreased LFP power at low and increased power at higher frequencies in mPFC and BLA across the dose range tested, although only data for the highest dose of FG-7142 are shown. In mPFC, the log ratio test indicated that FG-7142 significantly decreased power at low (<1 Hz) frequencies and significantly increased power in the delta (1–4 Hz), theta (4–8 Hz) and alpha (8–12 Hz) bands, compared with vehicle ($P < 0.05$). Similarly, in BLA, FG-7142 significantly decreased power at low (<1 Hz) frequencies whereas power was significantly increased in the theta band, compared with vehicle ($P < 0.05$). These changes in power most likely indicate a shift in the pattern of LFP activity from the irregular, higher amplitude deflections in potential seen in response to vehicle, to the more oscillatory, lower amplitude deflections in potential observed in response to FG-7142 (Fig. 2).

FG-7142 disrupts the functional connectivity within and between mPFC and BLA

Figure 6 shows the effects of FG-7142 on unit coherence, within mPFC or BLA and between mPFC and BLA. FG-7142 had little or no effect on unit coherence at the lowest dose tested (data not shown),
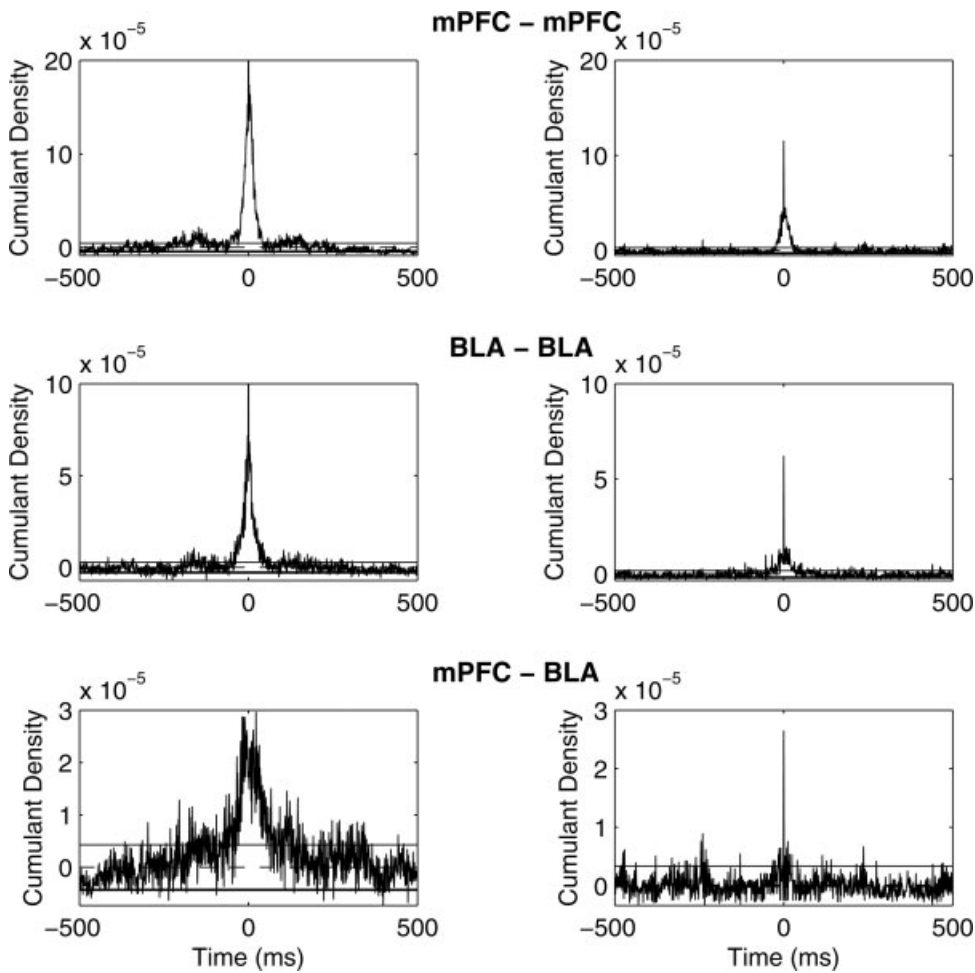
Fig. 7. Effects of FG-7142 on unit cumulant density. The solid horizontal lines at the bottom of the plots are the upper and lower 95% confidence limits, based on the assumption of independence. Units within mPFC or BLA showed significant cumulant densities in response to vehicle (left column). FG-7142 decreased unit cumulant density within mPFC or BLA (right column; data for lower doses of FG-7142 not shown). Cumulant density between mPFC and BLA units was also significant in response to vehicle; however, FG-7142 abolished the cumulant density between mPFC and BLA units.

whereas higher doses decreased unit coherence within and between PFC and BLA (only data for the highest dose of FG-7142 are shown). Units within mPFC or BLA displayed coherence across the frequency range (0–15 Hz) in response to vehicle ($P <$ 0.05), indicating that unit firing was linearly related in each of these regions. Coherence between mPFC and BLA units was also observed at lower frequencies (0–8 Hz) in response to vehicle ($P <$ 0.05). Comparison of coherence tests indicated that FG-7142 significantly attenuated unit coherence within mPFC or BLA, compared with vehicle ($P <$ 0.05). Moreover, there was no significant coherence between mPFC and BLA units in response to FG-7142, indicating a loss of synchronization of unit firing between these regions.

The effects of FG-7142 on unit cumulant density in mPFC and BLA are displayed in Figure 7. Again, there were no effects of FG-7142 on cumulant density within or between mPFC and BLA at the lowest dose tested (data not shown); however, higher doses of FG-7142 decreased cumulant density (only data for highest dose are shown). As was the case with coherence,

units within mPFC or BLA showed significant cumulant densities in response to vehicle ($P <$ 0.05), indicating a positive temporal relationship in unit firing within these regions. Qualitative analysis indicated that FG-7142 decreased unit cumulant density within mPFC or BLA. Cumulant density between mPFC and BLA units was also significant in response to vehicle ($P <$ 0.05). Again, as was the case with unit coherence, there was no significant cumulant density between mPFC and BLA units in response to FG-7142, also indicating a loss of synchronization in mPFC and BLA unit firing.

Figure 8 shows the effects of FG-7142 on LFP coherence and cumulant density. FG-7142 had similar effects on coherence and cumulant density between mPFC and BLA LFPs at each dose tested, although only data for highest dose are shown. In contrast to unit coherence, LFPs in mPFC and BLA showed coherence across the frequency range in response to vehicle. However, the comparison of coherence test did reveal that FG-7142 significantly decreased LFP coherence at low frequencies (<2 Hz), compared with vehicle ($P <$ 0.05). While mPFC and BLA LFPs
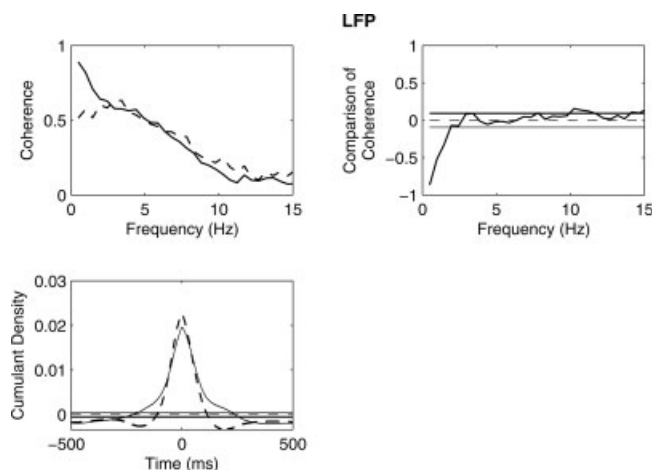
Fig. 8.   Effects of FG-7142 on LFP coherence and cumulant density. The solid and dashed lines correspond to vehicle and FG-7142, respectively, in the coherence and cumulant density plots (data for lower doses of FG-7142 not shown). LFPs in mPFC and BLA showed coherence across the whole frequency range in response to both vehicle and FG-7142 (upper right). However, the comparison of coherence test (upper right) revealed that FG-7142 significantly decreased LFP coherence at low frequencies (<2 Hz), compared with vehicle (vehicle is the reference in the comparison). Although LFPs in mPFC and BLA displayed significant cumulant densities in response to both vehicle and FG-7142 (lower plot), the cumulant density peak in response to FG-7142 was narrower and had additional negative components, reflecting enhanced oscillatory LFP activity.

showed significant cumulant densities in response to both vehicle and FG-7142, the cumulant density in response to FG-7142 had a more oscillatory form compared with vehicle, indicating an increase in the oscillatory activity in mPFC and BLA induced by FG-7142 (Fig. 2).

Effects of FLU on unit firing rate

From the results of the FG-7142 experiments it was apparent that this drug had different dose-related effects depending on the measure examined. For example, whereas FG-7142 increased unit activity only at the lowest dose (0.33 mg/kg) tested, the burst firing parameters and unit synchronization measures were only affected at higher doses. Given that the main objective of these experiments was to examine the effects of this drug on corticolimbic functional interactions, the FLU pretreatment experiments were conducted using the highest dose (10.0 mg/kg) of FG-7142 tested, despite the fact that this dose had no effect on unit firing rate.

The effects of FLU (1.0 mg/kg) on firing rate in mPFC and BLA are represented in Figure 9. In mPFC neurons, there was a significant main effect of drug in animals pretreated with FLU prior to FG-7142 (10.0 mg/kg) administration ($n = 31$, $F_{(2,30)} = 56.27$, $P < 0.0001$). Post hoc analysis revealed that

FLU significantly decreased mean firing rate, although there was no significant effect of FG-7142 on mean firing rate, compared with FLU. Similarly, in BLA neurons there was a significant main effect of drug in animals pretreated with FLU ($n = 26$, $F_{(2,25)} = 16.13$, $P < 0.0001$). As was the case in mPFC, post hoc analysis also revealed that FLU significantly decreased mean firing rate ($P < 0.05$). Again, there was no significant effect of FG-7142 on mean firing rate, compared with FLU.

FLU pretreatment blocks the effects of FG-7142 on burst firing parameters

Figure 10 depicts the effects of FLU pretreatment on FG-7142-induced changes in burst firing parameters in mPFC and BLA. In general, FLU pretreatment abolished the decrease in mPFC and BLA neuronal bursting that was expected in response to FG-7142 administration. However, FLU did decrease burst firing parameters in mPFC and BLA, compared with vehicle. There was a significant main effect of drug on the mean number of bursts/min ($F_{(2,30)} = 64.22$, $P < 0.0001$) and percentage of spikes firing in bursts ($F_{(2,30)} = 5.01$, $P < 0.01$) in mPFC neurons. Post hoc analysis revealed that, although FLU significantly decreased the mean number of bursts/min ($P < 0.05$) and percentage of spikes firing in bursts ($P < 0.05$), compared with vehicle, there was no significant effect of FG-7142, compared with FLU, on these two measures. Significant main effects of drug on the mean number of bursts/min ($F_{(2,25)} = 22.91$, $P < 0.0001$) and percentage of spikes firing in bursts ($F_{(2,25)} = 16.50$, $P < 0.0001$) were also seen in BLA neurons. Again, post hoc analysis revealed that FLU significantly decreased the mean number of bursts/min ($P < 0.05$) and percentage of spikes firing in bursts ($P < 0.05$), compared with vehicle, although there was no significant effect of FG-7142, compared with FLU, on either of these two measures. There was no significant main effect of drug on the mean number of spikes/burst in mPFC ($F_{(2,30)} = 0.76$, $P = 0.47$) or BLA ($F_{(2,25)} = 1.54$, $P = 0.23$).

FLU pretreatment abolishes the effects of FG-7142 on LFP activity

The effects of FLU pretreatment on FG-7142-induced alterations in LFP activity are shown in Figure 11. FLU decreased LFP power in both mPFC and BLA, compared with vehicle, over the entire frequency range. However, log ratio tests revealed little significant difference in power between FLU and FG-7142 at any frequency in either region, indicating that FLU pretreatment blocked the effects of FG-7412 on LFP activity in mPFC and BLA.
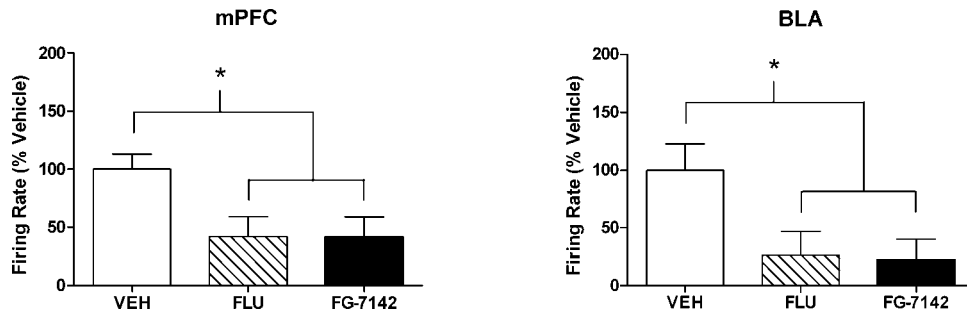
Fig. 9. Effects of FLU on firing rate. Although administration of FLU significantly decreased the mean firing rate in mPFC and BLA neurons, there was no significant difference in mean firing rate after administration of FG-7142 (10.0 mg/kg), compared with FLU (1.0 mg/kg) pretreatment (* VEH vs. FLU and FG-7142).
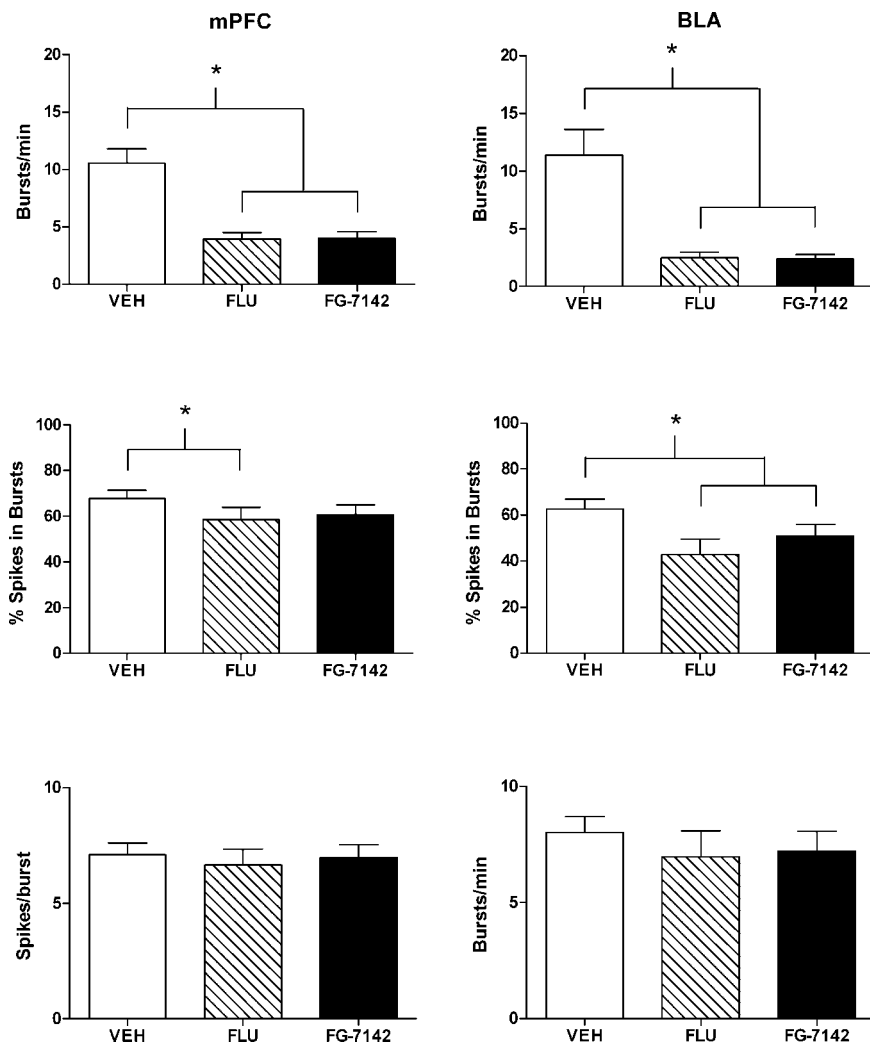

Fig. 10. Effects of FLU pretreatment on FG-7142-induced changes in burst firing. Administration of FLU significantly decreased the mean number of bursts/min (* VEH vs. FLU and FG-7142, $P < 0.05$) and percentage of spikes firing in bursts (* VEH vs. FLU, $P < 0.05$) in mPFC. FLU had the same effect on the mean number of bursts/min (* VEH vs. FLU and FG-7142, $P < 0.05$) and percentage of spikes firing in bursts (* VEH vs. FLU and FG-7142, $P < 0.05$) in BLA. There was no effect of FLU on the mean number of spikes/burst in mPFC or BLA. FG-7142 had no significant effect on any burst firing parameters in either region after FLU pretreatment.

FLU pretreatment blocks FG-7142-induced disruption of synchronization within and between mPFC and BLA

Figure 12 depicts the effects of FLU pretreatment on FG-7142-induced changes in unit coherence. Comparison of coherence tests revealed no significant

difference in coherence in response to FG-7142 and FLU, within mPFC or BLA and between mPFC and BLA, indicating that pretreatment with FLU abolished the effects of FG-7142 on unit coherence.

The effects of pretreatment with FLU on changes in unit cumulant density induced by FG-7142 are
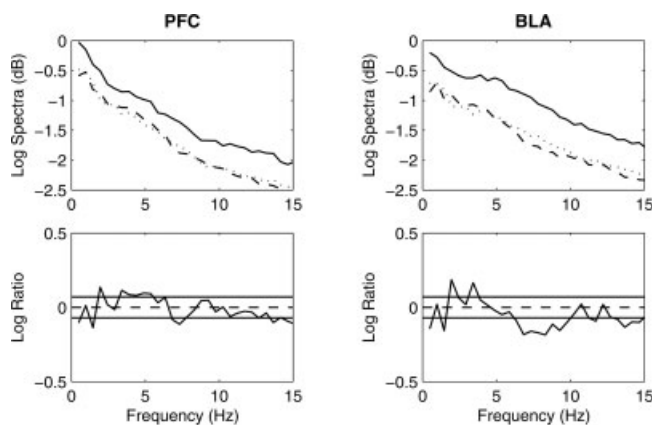
Fig. 11. Effects of FLU pretreatment on FG-7142-induced changes in LFP activity. Vehicle, FLU and FG-7142 are represented by solid, dotted, and dashed lines, respectively, in the power spectral estimates (upper plots). Although FLU decreased LFP power in mPFC and BLA, compared with vehicle, log ratio tests revealed little significant change in power in response to FG-7142 after pretreatment with FLU (lower plots; FLU is the reference in the comparison).

represented in Figure 13. Although FLU decreased cumulant density, within mPFC or BLA and between mPFC and BLA, there was no effect of FG-7142 after FLU pretreatment. Thus, prior administration with FLU blocked the effects of FG-7142 on unit cumulant density.

Figure 14 shows the effects of FLU pretreatment on changes in LFP coherence and cumulant density induced by FG-7142. As was the case for unit coherence, the comparison of coherence test revealed no significant effect of FG-7142 on LFP coherence when administered after pretreatment with FLU. This indicates that FLU pretreatment abolished the effects of FG-7142 on LFP coherence. FLU decreased LFP cumulant density, although there was no effect of FG-7142, compared with FLU, on this measure. Again, this indicates that the effects of FG-7142 on LFP cumulant density are blocked by pretreatment with FLU.

DISCUSSION

In the present study, in vivo electrophysiology was used to examine the effects of systemic administration of FG-7142, a benzodiazepine receptor partial inverse agonist, on mPFC and BLA activity in the anesthetized rat. This drug increased neuronal firing rates in both mPFC and BLA at the lowest dose tested. Conversely, various burst firing parameters in these regions were decreased with higher doses of FG-7142. LFPs in mPFC and BLA were also altered by FG-7142, inducing a change in pattern from irregular to oscillatory activity. LFP power was decreased at the lowest frequencies (<1 Hz) in both regions and

increased at higher frequencies in mPFC (1–12 Hz) and BLA (4–8 Hz). Interestingly, FG-7142 attenuated the functional coupling of neuronal activity within each of these two regions and diminished synchronized LFP activity between mPFC and BLA. Moreover, the synchronization of unit activity between mPFC and BLA was completely disrupted by FG-7142. These results indicate that systemic FG-7142 administration disrupts the functional connectivity both within and between mPFC and BLA. Given that FG-7142 mimics several behavioral (Birnbaum et al., 1999; File et al., 1982, 1985; Murphy et al., 1996; Pellow and File, 1986), neuroendocrine (Pellow and File, 1985; Stephens et al., 1987) and autonomic (Berntson et al., 1996; Hart et al., 1998) stress responses modulated by mPFC and BLA (Buijs and van Eden, 2000), it is tempting to speculate that disruption of neuronal network interactions within and between these regions may model certain aspects of corticolimbic dysfunction induced by stressors.

The observation that FG-7142 administration increased neuronal firing rate in mPFC and BLA may not be surprising as benzodiazepine receptor partial inverse agonism would be expected to decrease inhibition mediated by local GABA interneurons and, consequently, disinhibit activity in pyramidal neurons (Palmer et al., 1988). However, it remains unclear why only the lowest dose of FG-7142 increased neuronal activity. However, it is possible that the distinct subtypes of GABA interneurons present in mPFC (Gabbott et al., 1997; Kawaguchi and Kondo, 2002; Kawaguchi and Kubota, 1997) and BLA (McDonald and Mascagni, 2001, 2002, 2004; Muller et al., 2003; McDonald et al., 2004) are involved in mediating this dose-related increase in unit firing. FG-7142 also elevates monoamine metabolism in mPFC and BLA (Bradberry et al., 1991; Dazzi et al., 2002; Ida et al., 1991) and evidence indicates that monoamines can attenuate unit firing rate in these regions (Mantz et al., 1988; Nakano et al., 1987; Rosenkranz and Grace, 1999; Sesack and Bunney, 1989). Thus, it is possible that low doses of FG-7142 increase neuronal activity by a direct $GABA_A$ receptor-mediated mechanism of action, whereas higher doses of drug may have opposing effects on neuronal firing by acting both directly and indirectly via monoamine receptor activation. In addition to its effects on monoamine neurotransmission, this drug also induces glucocorticoid release (Pellow and File, 1985; Stephens et al., 1987). Previous studies indicate that corticosterone alters neuronal activity in mPFC (Jackson and Moghaddam, 2005) and BLA (Feldman et al., 1983), raising the possibility that FG-7142 exerts its effects on mPFC and BLA activity indirectly via glucocorticoid receptor activation. However, this explanation does not account for the dose-related effects of FG-7142 on unit activity observed in this report.
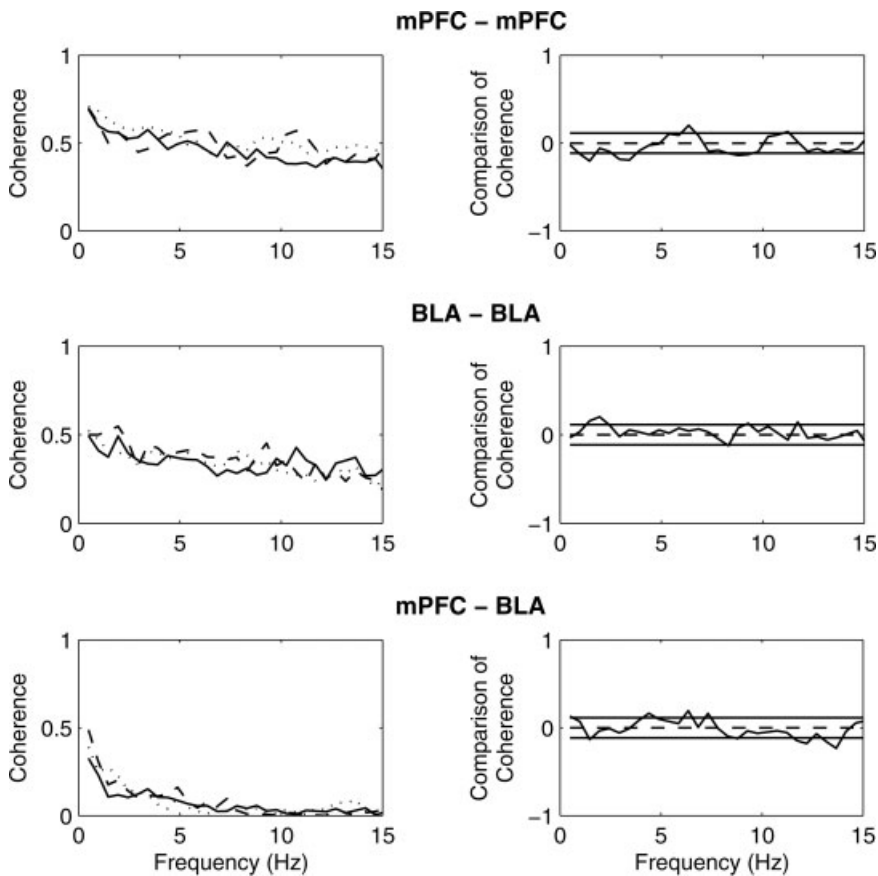
mPFC – mPFC

BLA – BLA

mPFC – BLA

Fig. 12. Effects of FLU pretreatment on FG-7142-induced changes in unit coherence. The solid, dotted, and dashed lines correspond to vehicle, FLU and FG-7142, respectively, in the coherence plots (left column). Comparison of coherence tests revealed no significant difference in coherence in response to FG-7142 after FLU pretreatment, within mPFC or BLA and between mPFC and BLA (right column; with FLU as the reference).

In contrast to the lack of effect on neuronal firing rate, higher doses of FG-7142 changed the pattern of unit firing in mPFC and BLA, resulting in attenuated burst firing parameters in these regions. Neuronal burst firing is thought to play an important role in information processing by enhancing synaptic transmission via increased neurotransmitter release and synaptic plasticity. Furthermore, it is hypothesized that information conveyed by bursts is qualitatively different from that of single spike firing (Cooper, 2002), such that certain burst firing parameters may mediate selective communication between neurons (Krahe and Gabbiani, 2004). Burst firing in mPFC is diminished by systemic administration of NMDA receptor antagonists, drugs which also disrupt working memory (Homayoun et al., 2005; Jackson et al., 2004). Given that NMDA receptor hypofunction and FG-7142 treatment have similar effects on mPFC bursting and working memory (Birnbaum et al., 1999; Murphy et al., 1996), burst firing in mPFC may play a critical role in mediating cognitive functions such as attention and vigilance (Krahe and Gabbiani, 2004). Similarly, amygdaloid bursts occur in response to affectively relevant stimuli (Nishijo et al., 1988). Moreover, bursting in individual BLA neurons may facilitate synaptic transmission in neighboring cells

and thus promote burst firing in populations of excitatory projection neurons (Paré et al., 1995).

The alterations in FG-7142-induced LFP activity seen in the present study are similar to those reported in previous studies. This drug increases LFP power in the delta (1–4 Hz) and theta (4–8 Hz) bands in various cortical regions, an effect blocked with FLU coadministration (Ehlers et al., 1990; Massotti, 1985; Massotti et al., 1985). Interestingly, as well as impairing working memory and burst firing in mPFC, systemic administration of NMDA receptor antagonists also increases LFP power in the delta band in this region (Sebban et al., 2002). Therefore, altered LFP activity in mPFC may represent another common mechanism by which cognitive function is perturbed. Conversely, increased theta band power in amygdala occurs in response to conditioned stress, suggesting that LFP activity in this region may facilitate consolidation of aversive learning by promoting synaptic plasticity (Paré et al., 2002).

The positive temporal relationship between activity in mPFC and BLA neurons observed in the present study is also in general agreement with the results of a recent study (Likhtik et al., 2005) and may occur as a result of the direct reciprocal projections between these regions (McDonald, 1991, 1998). However, the
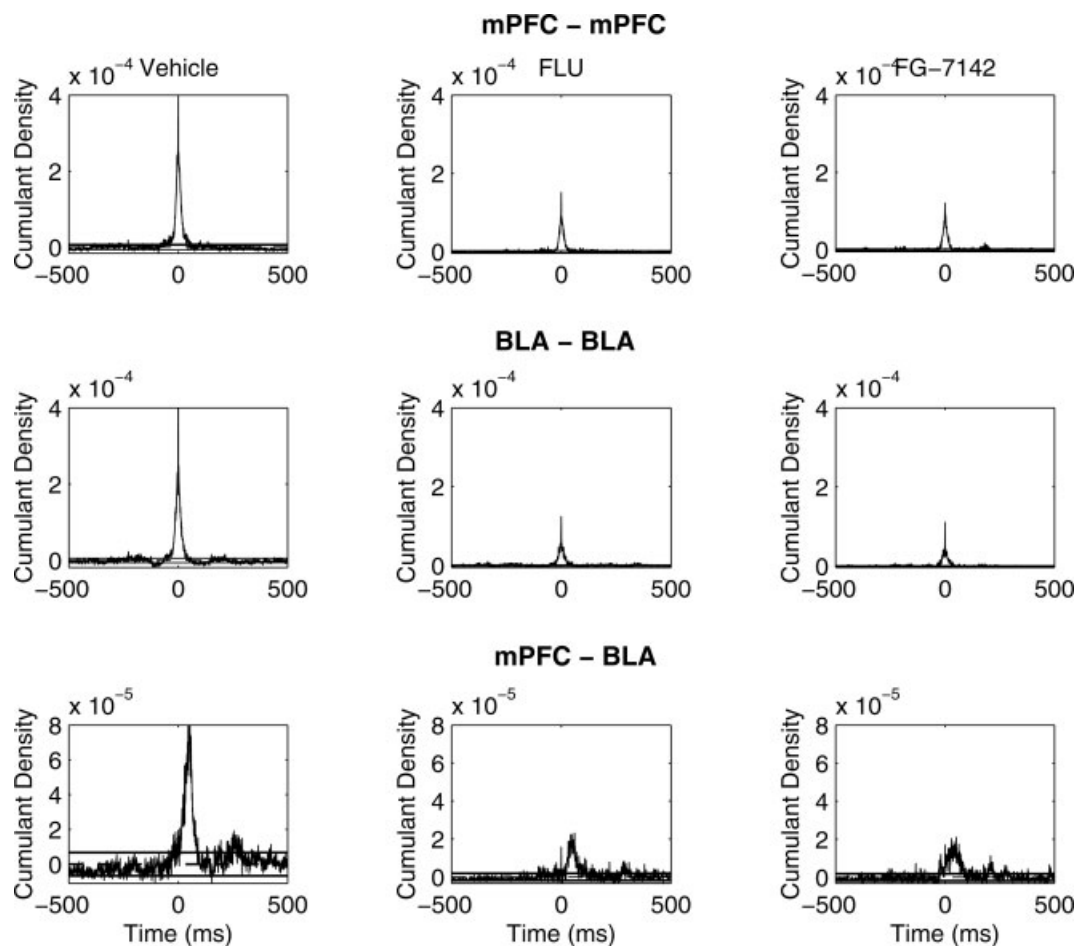
Fig. 13. Effects of FLU pretreatment on FG-7142-induced changes in unit cumulant density. Although FLU decreased cumulant density, both within and between mPFC and BLA, there was no effect of FG-7142 after prior administration with FLU.

BLA and mPFC also receive common sources of afferent input from thalamus (Krettek and Price, 1977; Ray and Price, 1992), hippocampus (Ishikawa and Nakamura, in press) and monoamine cell bodies (Fallon et al., 1978; Oades and Halliday, 1987; Room et al., 1981). Therefore these regions are also likely to contribute to the pattern of correlated activity between neurons in mPFC and BLA observed in this report.

Functional interactions between mPFC and BLA also appear to be relevant in processing sensory information associated with stressors. Electrical stimulation of mPFC suppresses both neuronal activity and plasticity in BLA induced by conditioned stressors (Rosenkranz et al., 2003). Conditioned stress also increases spontaneous activity and burst firing in a subpopulation of mPFC neurons which receive input from BLA, an effect which is abolished by BLA inactivation. These results suggest that both descending corticoamygdaloid and ascending amygdalocortical pathways play a critical role in forming affectively

significant associations during aversive learning (Laviolette et al., 2005). Interestingly, prior acute or chronic stress interferes with the subsequent extinction of fear conditioning or the recall of extinction learning (Izquierdo et al., 2006; Miracle et al., 2006), processes mediated by both mPFC (Milad and Quirk, 2002; Morgan and LeDoux, 1995; Quirk et al., 2000) and BLA (Chhatwal et al., 2005; Falls et al., 1992; Walker et al., 2002). Thus, the FG-7142-induced disruption of synchronized activity within and between mPFC and BLA reported in the present study may provide a useful model for examining the effects of stressors on corticolimbic interactions. However, given the ubiquitous nature of benzodiazepine receptor expression in the central nervous system (Mugnaini and Oertel, 1985), the effects of systemic FG-7142 administration should be interpreted with caution. Future experiments comparing the effects of systemic and intracerebral administration of FG-7142 on mPFC-BLA functional interactions should prove useful in clarifying this issue.
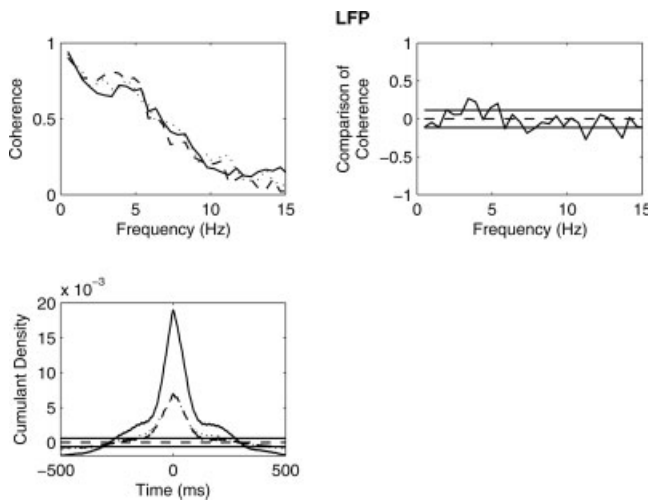
Fig. 14. Effects of FLU pretreatment on FG-7142-induced changes in LFP coherence and cumulant density. The solid, dotted, and dashed lines in the coherence graph (upper left) correspond to vehicle, FLU and FG-7142, respectively. The comparison of coherence test (upper right) revealed little significant difference in coherence in response to FG-7142 after FLU pretreatment. Similarly, although FLU decreased cumulant density (lower plot), there was no effect of FG-7142 after prior administration with FLU.

Functional imaging studies in humans have also demonstrated functional coupling between frontal cortex and amygdala in healthy individuals, both at rest (Zald et al., 1998) and during emotional processing tasks (Winston et al., 2003). Interestingly, presentation of aversive olfactory stimuli reduces interhemispheric functional coupling within frontal cortex and amygdala, as well as intrahemispheric functional coupling between these regions (Zald et al., 1998). Moreover, it has been hypothesized that dysfunctional frontocortical-amygdaloid connectivity may underlie the alterations in mPFC and amygdaloid function observed in mood disorders (Davidson et al., 2002; Irwin et al., 2004).

In planning the FLU pretreatment experiments, it was not initially apparent which dose of FG-7142 to use given the different dose-related effects FG-7142 had on the various activity and synchrony measures examined. Whereas FG-7142 increased unit activity only at the lowest dose (0.33 mg/kg) tested, the burst firing parameters and unit synchronization measures were only affected at higher doses. The primary objective of this study was to examine the effects of FG-7142 on corticolimbic functional interactions. Thus, the FLU pretreatment experiments were conducted using the highest dose (10.0 mg/kg) of FG-7142 tested, despite the fact that this dose had no effect on unit firing rate.

The effects of FG-7142 on burst firing, LFP activity, and both unit and LFP synchronization observed in this study were blocked with prior systemic administration of FLU, a selective benzodiazepine receptor antagonist. This suggests that the effects of FG-7142 reported in the present study were mediated via partial inverse agonism of the benzodiazepine receptor. FLU alone, however, attenuated neuronal firing rate, selected bursting parameters and LFP power in both mPFC and BLA. At first glance these effects may seem unexpected given that partial inverse agonism by FG-7142 and antagonism by FLU would both be expected to disinhibit pyramidal cells in mPFC and BLA. However, closer scrutiny of the literature regarding the mechanisms of action attributed to FLU indicates that this drug is not a "pure" antagonist but rather acts as a partial agonist at the benzodiazepine receptor (Brtitton et al., 1988; Buldakova and Weiss, 1997; Dantzer and Perio, 1982; Marescaux et al., 1984; Nutt et al., 1982; Obradovic et al., 2003; Pellow et al., 1984; Polc et al., 1995).

Examination of the lack of effects of FG-7142 on selected burst firing parameters, LFP power and both unit and LFP cumulant density after FLU pretreatment suggest the possibility of a floor effect. FLU pretreatment may not have blocked the effects of FG-7142 on these measures but rather decreased them so much that a further decrease after FG-7142 administration would not be possible. However, FLU alone did not affect other measures, such as bursts/min and both unit and LFP coherence, but FG-7142 had no effect when administered after FLU pretreatment, suggesting that FLU blocked the effects of FG-7142 on at least some of the measures examined.

In the present study, FG-7142 increased mPFC and BLA unit firing at the lowest dose tested and decreased burst firing at higher doses in these regions. FG-7142 also diminished LFP power at low frequencies and enhanced power at higher frequencies in mPFC and BLA. Importantly, FG-7142 attenuated synchronized unit firing, within and between mPFC and BLA. LFP synchronization between these areas was also decreased by FG-7142. Finally, FLU pretreatment blocked the changes in burst firing, LFP power, and synchronization of both unit and LFP activity induced by FG-7142. Studies conducted in the future comparing the effects of conventional stressors and FG-7142 on the functional connectivity between mPFC and BLA will be useful to confirm the validity of using FG-7142 to model the effects of stress on corticolimbic network interactions. The effects of isoflurane, the anesthetic used in the present study, are mediated in part by potentiating cortical (Hentschke et al., 2005) and amygdaloid (Ranft et al., 2004) GABA$_A$ receptor function, the site of benzodiazepine binding and action of FG-7142 and FLU. Thus, future experiments conducted in the freely-behaving animal will avoid the potential confound of drug interactions between isoflurane, FG-7142 and/or FLU.

ACKNOWLEDGMENTS

REFERENCES

Amjad AM, Halliday DM, Rosenberg JR, Conway BA. 1997. An extended difference of coherence test for comparing and combining several independent coherence estimates: Theory and application to the study of motor units and physiological tremor. J Neurosci Methods 73:69–79.

Battaglia M, Ogliari A. 2005. Anxiety and panic: From human studies to animal research and back. Neurosci Biobehav Rev 29:169–179.

Beck CH, Fibiger HC. 1995. Conditioned fear-induced changes in behavior and in the expression of the immediate early gene c-fos: With and without diazepam pretreatment. J Neurosci 15:709–720.

Berntson GG, Hart S, Ruland S, Sarter M. 1996. A central cholinergic link in the cardiovascular effects of the benzodiazepine receptor partial inverse agonist FG 7142. Behav Brain Res 74:91–103.

Birnbaum S, Gobeske KT, Auerbach J, Taylor JR, Arnsten AF. 1999. A role for norepinephrine in stress-induced cognitive deficits: α-1-adrenoceptor mediation in the prefrontal cortex. Biol Psychiatry 46:1266–1274.

Boraud T, Bezard E, Bioulac B, Gross CE. 2002. From single extracellular unit recording in experimental and human Parkinsonism to the development of a functional concept of the role played by the basal ganglia in motor control. Prog Neurobiol 66:265–283.

Bradberry CW, Lory JD, Roth RH. 1991. The anxiogenic β-carboline FG 7142 selectively increases dopamine release in rat prefrontal cortex as measured by microdialysis. J Neurochem 56:748–752.

Britton KT, Lee G, Koob GF. 1988. Corticotropin releasing factor and amphetamine exaggerate partial agonist properties of benzodiazepine antagonist Ro 15-1788 in the conflict test. Psychopharmacology 94:306–311.

Buijs RM, van Eden CG. 2000. The integration of stress by the hypothalamus, amygdala and prefrontal cortex: Balance between the autonomic nervous system and the neuroendocrine system. Prog Brain Res 126:117–132.

Buldakova S, Weiss M. 1997. Electrophysiological evidence for agonist properties of flumazenil, a benzodiazepine receptor antagonist, in rat hippocampus slices. J Neurol Sci 149:121–126.

Bullock T. 1997. Signals and signs in the nervous system: The dynamic anatomy of electrical activity is probably information-rich. Proc Natl Acad Sci USA 94:1–6.

Chhatwal JP, Myers KM, Ressler KJ, Davis M. 2005. Regulation of gephyrin and GABAA receptor binding within the amygdala after fear acquisition and extinction. J Neurosci 25:502–506.

Cocatre-Zielgien JH, Delcomyn F. 1992. Identification of bursts in spike trains. J Neurosci Methods 41:19–30.

Collins DR, Pelletier JG, Paré D. 2001. Slow and fast (γ) neuronal oscillations in the perirhinal cortex and lateral amygdala. J Neurophysiol 85:1661–1672.

Cooper B. 2001. Nature, nurture and mental disorder: old concepts in the new millennium. Br J PsychiatrySuppl 40:S91–S101.

Cooper DC. 2002. The significance of action potential bursting in the brain reward circuit. Neurochem Int 41:333–340.

Dantzer R, Perio A. 1982. Behavioural evidence for partial agonist properties of RO 15-1788, a benzodiazepine receptor antagonist. Eur J Pharmacol 81:655–658.

Davidson RJ, Pizzagalli D, Nitschke JB, Putnam K. 2002. Depression: Perspectives from affective neuroscience. Annu Rev Psychol 53:545–574.

Dazzi L, Ladu S, Spiga F, Vacca G, Rivano A, Pira L, Biggio G. 2002. Chronic treatment with imipramine or mirtazapine antagonizes stress- and FG7142-induced increase in cortical norepinephrine output in freely moving rats. Synapse 43:70–77.

Diggle PJ. 1990.Spectral analysis. In: Diggle PJ, editor. Time series. A biostatistical introduction. New York: Oxford University Press. p 94–133.

Drevets WC. 2001. Neuroimaging and neuropathological studies of depression: Implications for the cognitive-emotional features of mood disorders. Curr Opin Neurobiol 11:240–249.

Duncan GE, Johnson KB, Breese GR. 1993. Topographic patterns of brain activity in response to swim stress: Assessment by 2-deoxy-glucose uptake and expression of Fos-like immunoreactivity. J Neurosci 13:3932–3943.

Ehlers CL, Chaplin RI, Koob GF. 1990. EEG effects of Ro 15-4513 and FG 7142 alone and in combination with ethanol. Pharmacol Biochem Behav 36:607–611.

Fallon JH, Koziell DA, Moore RY. 1978. Catecholamine innervation of the basal forebrain. II. Amygdala, suprarhinal cortex and entorhinal cortex. J Comp Neurol 180:509–532.

Falls WA, Miserendino MJD, Davis M. 1992. Extinction of fear-potentiated startle: Blockade by infusion of an NMDA antagonist into the amygdala. J Neurosci 12:854–863.

Feldman S, Papir-Kricheli D, Dafny N. 1983. Single-cell and multiunit activity in freely moving rats after corticosterone administration. Exp Neurol 80:427–438.

File SE, Lister RG, Nutt DJ. 1982. The anxiogenic action of benzodiazepine antagonists. Neuropharmacology 21:1033–1037.

File SE, Pellow S, Braestrup C. 1985. Effects of the β-carboline, FG 7142, in the social interaction test of anxiety and the holeboard: Correlations between behaviour and plasma concentrations. Pharmacol Biochem Behav 22:941–944.

Gabbott PL, Dickie BG, Vaid RR, Headlam AJ, Bacon SJ. 1997. Local-circuit neurones in the medial prefrontal cortex (areas 25, 32 and 24b) in the rat: morphology and quantitative distribution. J Comp Neurol 377:465–499.

Garcia R, Vouimba RM, Baudry M, Thompson RF. 1999. The amygdala modulates prefrontal cortex activity relative to conditioned fear. Nature 402:294–296.

Gilboa A, Shalev AY, Laor L, Lester H, Louzoun Y, Chisin R, Bonne O. 2004. Functional connectivity of the prefrontal cortex and the amygdala in posttraumatic stress disorder. Biol Psychiatry 55:263–272.

Green JD. 1958. A simple microelectrode for recording from the central nervous system. Nature 182:962.

Gronier BS, Rasmussen K. 2003. Electrophysiological effects of acute and chronic olanzapine and fluoxetine in the rat prefrontal cortex. Neurosci Lett 349:196–200.

Halliday DM, Rosenberg JR, Amjad AM, Breeze P, Conway BA, Farmer SF. 1995. A framework for the analysis of mixed time series/point process data—Theory and application to the study of physiological tremor, single motor unit discharges and electromyograms. Prog Biophys Mol Biol 64:237–278.

Hart S, Sarter M, Bernston GG. 1998. Cardiovascular and somatic startle and defense: Concordant and discordant actions of benzodiazepine receptor agonists and inverse agonists. Behav Brain Res 90:175–186.

Hentschke H, Schwarz C, Antkowiak B. 2005. Neocortex is the major target of sedative concentrations of volatile anaesthetics: Strong depression of firing rates and increase of GABA-A receptor-mediated inhibition. Eur J Neurosci 21:93–102.

Homayoun H, Jackson ME, Moghaddam B. 2005. Activation of metabotropic glutamate 2/3 receptors reverses the effects of NMDA receptor hypofunction on prefrontal cortex unit activity in awake rats. J Neurophysiol 93:1989–2001.

Ida Y, Elsworth JD, Roth RH. 1991. Anxiogenic β-carboline FG 7142 produces activation of noradrenergic neurons in specific brain regions of rats. Pharmacol Biochem Behav 39:791–793.

Irwin W, Anderle MJ, Abercrombie HC, Schaefer SM, Kalin NH, Davidson RJ. 2004. Amygdalar interhemispheric functional connectivity differs between the non-depressed and depressed human brain. Neuroimage 21:674–686.

Ishikawa A, Nakamura S. 2006. Ventral hippocampal neurons project axons simultaneously to the medial prefrontal cortex and amygdala in the rat. J Neurophysiol 96:2134–2138.

Izquierdo A, Wellman CL, Holmes A. 2006. Brief uncontrollable stress causes dendritic retraction in infralimbic cortex and resistance to fear extinction in mice. J Neurosci 26:5733–5738.

Jackson ME, Moghaddam B. 2005. Glucocorticoid receptor activation disrupts oscillatory interactions between prefrontal cortex and hippocampus: Unit activity and local field potential recordings in awake rats. Soc Neurosci Abstr 889.11.

Jackson ME, Homayoun H, Moghaddam B. 2004. NMDA receptor hypofunction produces concomitant firing rate potentiation and burst activity reduction in the prefrontal cortex. Proc Natl Acad Sci USA 101:8467–8472.

Jung M, Qin Y, McNaughton B, Barnes C. 1998. Firing characteristics of deep layer neurons in prefrontal cortex in rats performing spatial working memory tasks. Cereb Cortex 8:437–450.

Kaneoke Y, Vitek JL. 1996. Burst and oscillation as disparate neuronal properties. J Neurosci Methods 68:211–223.

Kawaguchi Y, Kondo S. 2002. Parvalbumin, somatostatin and cholecystokinin as chemical markers for specific GABAergic interneuron types in the rat frontal cortex. J Neurocytol. 31:277–287.

Kawaguchi Y, Kubota Y. 1997. GABAergic cell subtypes and their synaptic connections in rat frontal cortex. Cereb Cortex 7:476–486.

Kim YB, Jang J, Chung Y, Baeg EH, Kim HT, Mook-Jung I, Kim SU, Jung MW, Chung YK. 2001. Haloperidol and clozapine increase neural activity in the rat prefrontal cortex. Neurosci Lett 298:217–221.

Krahe R, Gabbiani F. 2004. Burst firing in sensory systems. Nat Rev Neurosci 5:13–24.

Krettek JE, Price JL. 1977. The cortical projections of the mediodorsal nucleus and adjacent thalamic nuclei in the rat. J Comp Neurol 171:157–191.

Kurumaji A, Umino A, Tanami M, Ito A, Asakawa M, Nishikawa T. 2003. Distribution of anxiogenic-induced c-Fos in the forebrain regions of developing rats. J Neural Transm 110:1161–1168.

Laviolette SR, Lipski WJ, Grace AA. 2005. A subpopulation of neurons in the medial prefrontal cortex encodes emotional learning with burst and frequency codes through a dopamine D4 receptor-dependent basolateral amygdala input. J Neurosci 25:6066–6075.

LeDoux JE. 2000. Emotion circuits in the brain. Annu Rev Neurosci 23:155–184.

Legendy CR, Salcman M. 1985. Bursts and recurrences of bursts in the spike trains of spontaneously active striate cortex neurons. J Neurophysiol 53:926–939.

Likhtik E, Pelletier JG, Paz R, Paré D. 2005. Prefrontal control of the amygdala. J Neurosci 25:7429–7437.

Mantz J, Milla C, Glowinski J, Thierry AM. 1988. Differential effects of ascending neurons containing dopamine and noradrenaline in the control of spontaneous activity and of evoked responses in the rat prefrontal cortex. Neuroscience 27:517–526.

Marescaux C, Micheletti G, Vergnes M, Depaulis A, Rumbach L, Warter JM. 1984. Biphasic effects of Ro 15-1788 on spontaneous petit mal-like seizures in rats. Eur J Pharmacol 102:355–359.

Maroun M, Richter-Levin G. 2003. Exposure to acute stress blocks the induction of long-term potentiation of the amygdala-prefrontal cortex pathway in vivo. J Neurosci 23:4406–4409.

Massotti M. 1985. Electroencephalographic investigations in rabbits of drugs acting at GABA-benzodiazepine-barbiturate/picrotoxin receptors complex. Pharmacol Biochem Behav 23:661–670.

Massotti M, Lucantoni D, Caporalli MG, Mele L, Gatta F. 1985. Supraspinal convulsions induced by inverse benzodiazepine agonists in rabbits. J Pharmacol Exp Ther 234:274–279.

McDonald AJ. 1991. Organization of amygdaloid projections to the prefrontal cortex and associated striatum in the rat. Neuroscience 44:1–14.

McDonald AJ. 1998. Cortical pathways to the mammalian amygdala. Prog Neurobiol 55:257–332.

McDonald AJ, Mascagni F. 2001. Colocalization of calcium-binding proteins and GABA in neurons of the rat basolateral amygdala. Neuroscience 105:681–693.

McDonald AJ, Mascagni F. 2002. Immunohistochemical characterization of somatostatin containing interneurons in the rat basolateral amygdala. Brain Res 943:237–244.

McDonald AJ, Mascagni F. 2004. Parvalbumin-containing interneurons in the basolateral amygdala express high levels of the $\alpha1$ subunit of the GABAA receptor. J Comp Neurol 473:137–146.

McDonald AJ, Mascagni F, Muller JF. 2004. Immunocytochemical localization of GABABR1 receptor subunits in the basolateral amygdala. Brain Res 1018:147–158.

McEwen BS. 2000. Allostasis and allostatic load: Implications for neuropsychopharmacology. Neuropsychopharmacology 22:108–124.

Milad MR, Quirk. 2002. Neurons in medial prefrontal cortex signal memory for fear extinction. Nature 420:70–74.

Miracle AD, Brace MF, Huyck KD, Singler SA, Wellman CL. 2006. Chronic stress impairs recall of extinction of conditioned fear. Neurobiol Learn Mem 85:213–218.

Morgan MA, LeDoux JE. 1995. Differential contribution of dorsal and ventral medial prefrontal cortex to the acquisition and extinction of conditioned fear in rats. Behav Neurosci 109:681–688.

Mugnaini E, Oertel WH. 1985. An atlas of the distribution of GABAergic neurons and terminals in the rat. In: Björklund A, Hökfelt T, editors. Handbook of chemical neuroanatomy, Vol. 4. Amsterdam: Elsevier. p 436–608.

Muller JF, Mascagni F, McDonald AJ. 2003. Synaptic connections of distinct interneuronal subpopulations in the rat basolateral amygdalar nucleus. J Comp Neurol 456:217–236.

Murphy BL, Arnsten AF, Jentsch JD, Roth RH. 1996. Dopamine and spatial working memory in rats and monkeys: Pharmacological reversal of stress-induced impairment. J Neurosci 16:7768–7775.

Nakano Y, Lenard L, Oomura Y, Nishino H, Aou S, Yamamoto T. 1987. Functional involvement of catecholamines in reward-related neuronal activity of the monkey amygdala. J Neurophysiol 57:72–91.

Nemeroff CB, Vale WW. 2005. The neurobiology of depression: Inroads to treatment and new drug discovery. J Clin Psychiatry Suppl 7:5–13.

Nishijo H, Ono T, Nishino H. 1988. Single neuron responses in amygdala of alert monkey during complex sensory stimulation with affective significance. J Neurosci 8:3570–3583.

Nutt DJ, Cowen PJ, Little HJ. 1982. Unusual interactions of benzodiazepine receptor antagonists. Nature 295:436–438.

Oades RD, Halliday GM. 1987. Ventral tegmental (A10) system: Neurobiology. 1. Anatomy and connectivity. Brain Res 434:117–165.

Obradovic DI, Savic MM, Andjelkovic DS, Ugresic ND, Bokonjic DR. 2003. The influence of midazolam and flumazenil on rat brain slices oxygen consumption. Pharmacol Res 47:127–131.

Palmer MR, van Horne CG, Harlan JT, Moore EA. 1988. Antagonism of ethanol effects on cerebellar Purkinje neurons by the benzodiazepine inverse agonists Ro 15-4513 and FG 7142: electrophysiological studies. J Pharmacol Exp Ther 247:1018–1024.

Paré D, Pape HC, Dong J. 1995. Bursting and oscillating neurons of the cat basolateral amygdaloid complex in vivo: Electrophysiological properties and morphological features. J Neurophysiol 74:1179–1191.

Paré D, Collins DR, Pelletier JG. 2002. Amygdala oscillations and the consolidation of emotional memories. Trends Cogn Sci 6:306–314.

Paxinos G, Watson C. 1997. The rat brain in stereotaxic coordinates. 3rd ed. New York: Academic Press.

Pellow S, File SE. 1985. The effects of putative anxiogenic compounds (FG 7142, CGS 8216 and Ro 15-1788) on the rat corticosterone response. Physiol Behav 35:587–590.

Pellow S, File SE. 1986. Anxiolytic and anxiogenic drug effects on exploratory activity in an elevated plus-maze: A novel test of anxiety in the rat. Pharmacol Biochem Behav 24:525–529.

Pellow S, File SE, Herberg LJ. 1984. Intracranial self-stimulation distinguishes between two benzodiazepine antagonists. Neurosci Lett 47:173–177.

Pérez-Jaranay JM, Vives F. 1991. Electrophysiological study of the response of medial prefrontal cortex neurons to stimulation of the basolateral nucleus of the amygdala in the rat. Brain Res 564:97–101.

Pistis M, Perra S, Pillolla G, Melis M, Gessa GL, Muntoni AL. 2004. Cannabinoids modulate neuronal firing in the rat basolateral amygdala: Evidence for CB1- and non-CB1-mediated actions. Neuropharmacology 46:115–125.

Polc P, Jahromi SS, Facciponte G, Pelletier MR, Zhang L, Carlen PL. 1995. Benzodiazepine antagonist flumazenil reduces hippocampal epileptiform activity. Neuroreport 6:1549–1552.

Ponomarenko AA, Korotkova TM, Haas HL. 2003. High frequency (200 Hz) oscillations and firing patterns in the basolateral amygdala and dorsal endopiriform nucleus of the behaving rat. Behav Brain Res 141:123–129.

Quirk GJ, Russo GK, Barron JL, Lebron K. 2000. The role of ventromedial prefrontal cortex in the recovery of extinguished fear. J Neurosci 20:6225–6231.

Ranft A, Kurz J, Deuringer M, Haseneder R, Dodt HU, Zieglgansberger W, Kochs E, Eder M, Hapfelmeier G. 2004. Isoflurane modulates glutamatergic and GABAergic neurotransmission in the amygdala. Eur J Neurosci 20:1276–1280.

Ray JP, Price JL. 1992. The organization of the thalamocortical connections of the mediodorsal thalamic nucleus in the rat, related to the ventral forebrain-prefrontal cortex topography. J Comp Neurol 323:167–197.

Robbins T. 2000. From arousal to cognition the integrative position of the prefrontal cortex. Prog Brain Res 126:469–483.

Robinson DA. 1968. The electrical properties of metal electrodes. Proc IEEE 56:1065–1071.

Room P, Postema F, Korf J. 1981. Divergent axon collaterals of rat locus coeruleus neurons: Demonstration by a fluorescent double labeling technique. Brain Res 221:219–230.

Rosenberg JR, Amjad AM, Breeze P, Brillinger DR, Halliday DM. 1989. The Fourier approach to the identification of functional coupling between neuronal spike trains. Prog Biophys Mol Biol 53:1–31.

Rosenkranz JA, Grace AA. 1999. Modulation of basolateral amygdala neuronal firing and afferent drive by dopamine receptor activation in vivo. J Neurosci 19:11027–11039.

Rosenkranz JA, Grace AA. 2001. Dopamine attenuates prefrontal cortical suppression of sensory inputs to the basolateral amygdala of rats. J Neurosci 21:4090–103.

Rosenkranz JA, Grace AA. 2002. Cellular mechanisms of infralimbic and prelimbic prefrontal cortical inhibition and dopaminergic modulation of basolateral amygdala neurons in vivo. J Neurosci 22:324–337.

Rosenkranz JA, Moore H, Grace AA. 2003. The prefrontal cortex regulates lateral amygdala neuronal plasticity and responses to previously conditioned stimuli. J Neurosci 23: 11054–11064.

Sebban C, Tesolin-Decros B, Ciprian-Ollivier J, Perret L, Spedding M. 2002. Effects of phencyclidine (PCP) and MK 801 on the EEGq in the prefrontal cortex of conscious rats; antagonism by clozapine, and antagonists of AMPA-, α1- and 5-HT2a-receptors. Brit J Pharmacol 135:65–78.

Sesack SR, Bunney BS. 1989. Pharmacological characterization of the receptor mediating electrophysiological responses to dopamine in the rat medial prefrontal cortex: A microiontophoretic study. J Pharmacol Exp Ther 248:1323–1333.

Shin LM, Orr SP, Carson MA, Rauch SL, Macklin ML, Lasko NB, Peters PM, Metzger LJ, Dougherty DD, Cannistraro PA, Alpert NM, Fischman AJ, Pitman RK. 2004. Regional cerebral blood flow in the amygdala and medial prefrontal cortex during traumatic imagery in male and female Vietnam veterans with PTSD. Arch Gen Psychiatry 61:168–176.

Singewald N, Salchner P, Sharp T. 2003. Induction of c-Fos expression in specific areas of the fear circuitry in rat forebrain by anxiogenic drugs. Biol Psychiatry 53:275–283.

Smith Y, Pare JF, Paré D. 2000. Differential innervation of parvalbumin-immunoreactive interneurons of the basolateral amygdaloid complex by cortical and intrinsic inputs. J Comp Neurol 416:496–508.

Snodderly DM Jr. 1973. Extracellular single unit recording. In: Thompson RF, Patterson MM, editors. Bioelectric recording techniques, Part A: Cellular processes and brain potentials. New York: Academic Press. p 137–163.

Stephens DN, Schneider HH, Kehr W, Jensen LH, Petersen E, Honore T. 1987. Modulation of anxiety by β-carbolines and other benzodiazepine receptor ligands: Relationship of pharmacological to biochemical measures of efficacy. Brain Res Bull 19:309–318.

Steriade M. 1997. Synchronized activities of coupled oscillators in the cerebral cortex and thalamus at different levels of vigilance. Cereb Cortex 7:583–604.

Walker DL, Ressler KJ, Lu KT, Davis M. 2002. Facilitation of conditioned fear extinction by systemic administration or intra-amygdala infusions of D-cycloserine as assessed with fear-potentiated startle in rats. J Neurosci 22:2343–2351.

Winston JS, O'Doherty J, Dolan RJ. 2003. Common and distinct neural responses during direct and incidental processing of multiple facial emotions. Neuroimage 20:84–97.

Zald DH, Donndelinger MJ, Pardo JV. 1998. Elucidating dynamic brain interactions with across-subjects correlational analyses of positron emission tomographic data: The functional connectivity of the amygdala and orbitofrontal cortex during olfactory tasks. J Cereb Blood Flow Metab 18:896–905.